

Finding efficient observable operators in entanglement detection via convolutional neural network

Zi-Qi Lian,¹ You-Yang Zhou,¹ Liu-Jun Wang,^{1,*} and Qing Chen^{1,†}

¹*School of Physics and Astronomy and Yunnan Key Laboratory for Quantum Information, Yunnan University, Kunming 650500, China*

In quantum information, it is of high importance to efficiently detect entanglement. Generally, it needs quantum tomography to obtain state density matrix. However, it would consumes a lot of measurement resources, and the key is how to reduce the consumption. In this paper, we discovered the relationship between convolutional layer of artificial neural network and the average value of an observable operator in quantum mechanics. Then we devise a branching convolutional neural network which can be applied to detect entanglement in 2-qubit quantum system. Here, we detect the entanglement of Werner state, generalized Werner state and general 2-qubit states, and observable operators which are appropriate for detection can be automatically found. Beside, compared with privious works, our method can achieve higher accuracy with fewer measurements for quantum states with specific form. The results show that the convolutional neural network is very useful for efficiently detecting quantum entanglement.

INTRODUCTION

Nowadays, Machine Learning has become a powerful tool in tackling some complicated quantum physics problems, beacuse of its ability to find potential patterns in vast data. The breakthroughs have been made in multi-particle quantum system state ansatz [1–13], discovering quantum phase transition [14–19], classifying quantum correlations [20–29], detecting entanglement structure [30] and estimating the violation of multi-particle Bell inequalities [31], etc. On the other hand, with the development of the quantum computer, scientists pay more attention to quantum Machine Learning algorithms, which will be implemented on quantum computer, such as quantum approximate optimization algorithm [32], variational quantum eigensolver [33], quantum Boltzmann machine [34], and quantum neural network [35, 36]. They will promote the development of Machine Learning.

Among complicated quantum physics problems, the detection of quantum entanglement is an essential one. Quantum entanglement is the essential resource in application of quantum teleportation [37], quantum key distribution [38] and quantum computation [39]. Although there are many entanglement detection criteria have been proposed such as positive partial transpose (PPT) criterion [40, 41], computable cross norm criterion or realignment [42, 43] and entanglement witnesses [44–48] etc, complete classifying entanglement is still an NP-hard problem [49].

Recent years, scientists have also done many researches on using machine learning to study quantum entanglement. For instance, based on deterministic measurement operators, artificial neural network can be used to classify the entanglement in 2-qubits or 3-qubits systems [20, 28]. Combined with supervised learning, convex hull approximation can sample a mass of separable pure state to

approximate the shape of separable states set [21]. Convolutional neural network (CNN) can estimate the entanglement entropy of disordered interacting quantum many-particle system [23]. And fully connected neural network (FC) can be used to predict the multipartite entanglement structure of states composed by random subsystems [30] or find semi-optimal measurements for entanglement detection [50].

In this work, we successfully applied CNN to detect entanglement. CNN is one of the most representative neural networks which is considered more efficient than FC [51]. At present, CNN has been used to express quantum state of multi-particle system [7–10], estimate entanglement entropy of quantum many-particle system [23] and the parameters of multi-particle Hamiltonian [52]. Here, we first show why the observable operator of quantum system with discrete energy levels can be regarded as a special convolution kernel and how to use a convolution kernel to represent an observable operator and get the average of the operators. Afterward, we prove that the Hermiticity of convolutional layers can maintain in the training course if the input and the kernels are initialized as Hermitian matrix.

Then, we devised branching convolutional neural network (BCNN) (depicted in Fig.3(c)) which has a number of independent convolutional pathes. Every convolutional path accurately calculates average value of observable operators in inputted quantum state. According to the features of quantum state, the structures of convolutional pathes, it can automatically find appropriate observable operators whitch can extract information required by training goal. Because of that, it can decrease resource consumption in practice. We detected the entanglement of 2-qubits state and research the influence of the number of observable operators on the accuracy of our model.

* ljwangq@ynu.edu.cn

† chenqing@ynu.edu.cn

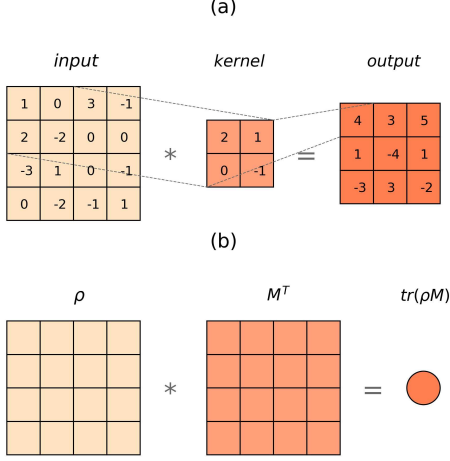


FIG. 1. (a), A example of convolution without bias and activation function. The step size of kernel equal to 1. (b), The convolutional layer with the input ρ and the kernel M^T , and its output is $tr(\rho M)$.

RESULTS

Regard observable operator as a kernel

CNN extract features from input data by the kernels, which are composed of trainable parameters. Every kernel scans the input data according to a certain step size. In each step, its parameters are multiplied with the corresponding input data and all are added as output. We can see a simple example of convolution without bias and activation function in Fig.1(a).

As we know, quantum states can completely describe a system. Observable operators can extract features such as momentum, spin, position, etc. from quantum states. From the point of feature extraction, we prove that the observable operator of discrete level system is a special convolution kernel. In Fig.1(b), we show how the convolutional layer can accurately calculate the average value of observable operator. We take state density matrix ρ as the input of the neural network and the transpose of observable operator M^T as the kernel, and the output of convolution without activation function and bias is

$$\begin{aligned} \rho * M^T &= \sum_{ij} \langle i | \left(\sum_{kl} \rho_{kl} M_{lk} |k\rangle \langle l| \right) |j\rangle \\ &= \sum_{ij} \rho_{ij} M_{ji} \\ &= \langle M \rangle, \end{aligned} \quad (1)$$

where $*$ means the convolution in the artificial neural network. If there are 2 subsystem with the dimension $d^{(1)}$ and $d^{(2)}$, its state density matrix can be written as $\rho =$

$\sum_{ij,kl} \rho_{ijkl} |i\rangle \langle j| \otimes |k\rangle \langle l|$ and the observable operator M can be written as $M = M^{(1)} \otimes M^{(2)}$. In the same way, we take $M^{(2)T}$ and $M^{(1)T}$ as the kernels of the first and the second convolutional layers, and their step sizes are exactly equal to their own dimensions. The output of the first convolutional layer is

$$\begin{aligned} O^{[1]} &= \rho * M^{(2)T} \\ &= \left(\sum_{ij,kl} \rho_{ijkl} |i\rangle \langle j| \otimes |k\rangle \langle l| \right) * M^{(2)T} \\ &= \sum_{ij,kl} \rho_{ij,kl} |i\rangle \langle j| \otimes (|k\rangle \langle l| * M^{(2)T}) \\ &= \sum_{ij} \sum_{kl} \rho_{ij,kl} \langle l | M^{(2)} |k\rangle |i\rangle \langle j| \\ &= tr_{(2)} \left(\rho \cdot I^{(1)} \otimes M^{(2)} \right). \end{aligned} \quad (2)$$

i.e., the first convolutional layer calculate the partial trace for the subsystem (2) of $\rho \cdot I^{(1)} \otimes M^{(2)}$, thus $O^{[1]}$ is Hermitian and its dimension is $d^{(1)}$. Then, the output of the second convolutional layer can be got as

$$\begin{aligned} O^{[2]} &= O^{[1]} * M^{(1)T} \\ &= \left(\rho * M^{(2)T} \right) * M^{(1)T} \\ &= tr_{(2)} \left(\rho \cdot I^{(1)} \otimes M^{(2)} \right) * M^{(1)T} \\ &= tr \left[\rho \cdot \left(M^{(1)} \otimes M^{(2)} \right) \right] \\ &= \langle M^{(1)} \otimes M^{(2)} \rangle. \end{aligned} \quad (3)$$

Similarly, suppose that there are N subsystems with dimension $d^{(1)}, d^{(2)}, \dots, d^{(N)}$, and the observable operator M can be written as $M = M^{(1)} \otimes M^{(2)} \otimes \dots \otimes M^{(N)}$, it is possible to calculate its average via the convolutional path with N convolutional layers. For $\forall n \leq N$, the kernel of the n -th convolutional layer is $M^{(N-n+1)T}$, and the step size equal to its dimensions. Therefore, for $\forall n < N$, the output $O^{[n]}$ is

$$\begin{aligned} O^{[n]} &= O^{[n-1]} * M^{(N-n+1)T} \\ &= tr_{(N-n+1)} \left(O^{[n-1]} \cdot I^{(1)} \otimes \dots \otimes I^{(N-n)} \right) \\ &\quad \otimes M^{(N-n+1)} \\ &= tr_{(N-n+1, \dots, N)} \left(\rho I^{(1)} \otimes \dots \otimes I^{(N-n)} \right) \\ &\quad \otimes M^{(N-n+1)} \otimes \dots \otimes M^{(N)}. \end{aligned} \quad (4)$$

Likewise, it can be prove that $O^{[n]}$ is also Hermitian, and its dimension is $d^{(O)} = d^{(1)} \cdot d^{(2)} \dots d^{(N-n)} = d^{(O')} \cdot d^{(M')}$, where $d^{(O')}$ and $d^{(M')}$ are the dimensions of the output $O^{(n+1)}$ and kernel $M^{(N-n)T}$ of next layer. In the same

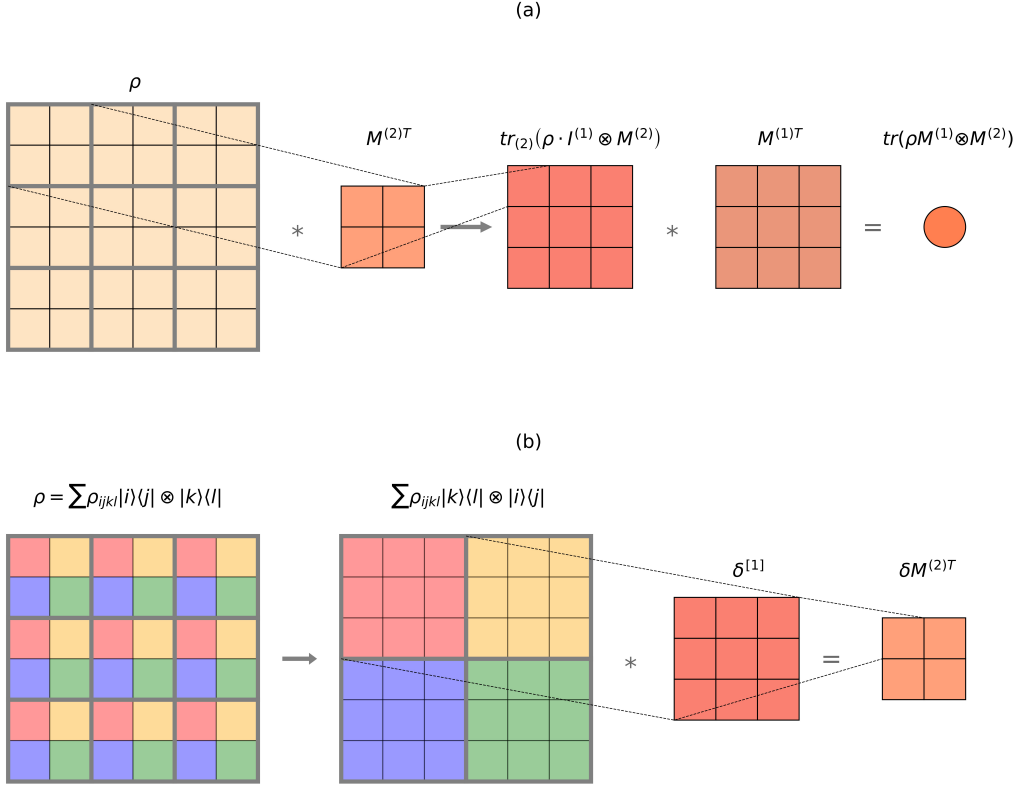


FIG. 2. Take the 3×2 system as an example. **(a)**, There are two convolutional layers without activation function and bias. The first layer has the kernel $M^{(2)T}$ and the input ρ . The second has the kernel $M^{(1)T}$. The output of the second convolutional layer is exactly equal to $\langle M^{(1)} \otimes M^{(2)} \rangle$. **(b)**, The gradient $\delta M^{(2)T}$ of the kernel $M^{(2)T}$ can be obtained by calculating convolution of $\sum \rho_{ijkl} |k\rangle\langle l| \otimes |i\rangle\langle j|$ and $\delta^{[1]}$, where $\sum \rho_{ijkl} |k\rangle\langle l| \otimes |i\rangle\langle j|$ can be obtained by swapping the corner labels of ρ and $\delta^{[1]}$ is the error propagated into the first convolutional layer.

way, the output of the last layer also can be obtained

$$\begin{aligned} O^{[N]} &= \left(\left(\left(\rho * M^{(N)T} \right) * M^{(N-1)T} \right) * \dots \right) * M^{(1)T} \\ &= \langle M^{(1)} \otimes M^{(2)} \otimes \dots \otimes M^{(N)} \rangle. \end{aligned} \quad (5)$$

Furthermore, considering that artificial neural networks are usually trained based on gradient descent, we prove that if the input and kernel of the convolutional layer are initialized as Hermitian matrixes, the gradient of the kernel will also be Hermitian. The calculation of kernel's gradient depends on the neural network error matrix from back propagation and the input of convolutional layer. We let $\delta^{[n]}$ be the error matrix which is propagated into the n -th convolutional layer. Its dimension always equal to dimension of $O^{[n]}$. Since the step size of the kernels here are equal to their dimensions, for $\forall n < N$, $\delta^{[n]}$ can be expressed as

$$\delta^{[n]} = \delta^{[n+1]} \otimes M^{(N-n)T}. \quad (6)$$

Because of the Hermiticity of $O^{[N]}$, the error $\delta^{[N]}$, which is propagated from the fully connected layer, must be a real number too. It means for $\forall n \leq N$, $\delta^{[n]}$ is Hermitian. Considering that, for $\forall n < N$, $d^{(O)} = d^{(O')} \cdot d^{(M')}$, so $O^{[n]}$ can be written as $\sum_{ij,kl}^{d^{(O')}, d^{(M')}} O_{ijkl}^{[n]} |i\rangle\langle j| \otimes |k\rangle\langle l|$. Then according to the neural network back propagation theory, for $\forall n \leq N$, the kernel gradient is

$$\begin{aligned} \delta M^{(N-n+1)T} &= \sum_{ij,kl}^{d^{(O')}, d^{(M')}} O_{ij,kl}^{[n-1]} |k\rangle\langle l| \otimes |i\rangle\langle j| * \delta^{[n]} \\ &= \sum_{kl}^{d^{(M')}} \sum_{ij}^{d^{(O')}} O_{ij,kl}^{[n-1]} \langle j | \delta^{[n]T} | i \rangle |k\rangle\langle l|. \end{aligned} \quad (7)$$

Since $O^{[n-1]}$ and $\delta^{[n]}$ are Hermitian, so $\sum_{ij} O_{ij,kl}^{[n-1]} \langle j | \delta^{[n]T} | i \rangle = (\sum_{ij} O_{ij,kl}^{[n-1]} \langle j | \delta^{[n]T} | i \rangle)^*$, as well as, $\delta M^{(N-n+1)T}$ is also Hermitian. Therefore, in the process of updating based on gradient descent, the

Hermiticity of the kernel will not change.

So far, we prove that the observable operator of the discrete level system can indeed be regarded as a special convolution kernel, the convolutional layer can be used to calculate the average of observable operators, and these convolutional layers can naturally keep Hermiticity when trained by gradient-based optimization methods.

Entanglement detection for 2-qubits state

Based on the content we introduced above, we devise the BCNN (depicted in Fig.3) to classify the entanglement of 2-qubits state. BCNN consists of several convolution paths and the following fully connected layers. It can automatically find proper observable operators which can extract information needed for the training goal. Here, we use $(m; n_1, n_2)$ to describe the structure of convolutional paths, where m means how many convolutional paths the network has, n_1 and n_2 means there are two layers of convolutional layer in a convolutional path and they have n_1 and n_2 kernels respectively. After training, the trained observable operators can be obtained from these kernels. More details of BCNN is introduced in the section Methods. Our dataset consists of state density matrixes and corresponding entanglement labels. The labels are determined by PPT criterion, which is necessary and sufficient for entanglement classification of 2×2 and 2×3 system [53]. Next, we will briefly introduce the quantum states we tested. The Werner state is

$$\rho = p|\psi\rangle\langle\psi| + \frac{(1-p)I}{4}, \quad (8)$$

where, $|\psi\rangle = \frac{1}{\sqrt{2}}(|00\rangle + |11\rangle)$, $p \in (0, 1)$. It has only one free parameter p , when $p > \frac{1}{3}$ it is entangled [54].

The first generalized Werner state which we called GI-Werner state is

$$\rho(\theta) = p|\psi_\theta\rangle\langle\psi_\theta| + \frac{(1-p)I_A}{2} \otimes \rho_B^\theta, \quad (9)$$

where, $|\psi_\theta\rangle = \cos\theta|00\rangle + \sin\theta|11\rangle$, $p \in (0, 1)$, $\theta \in (0, 2\pi)$, and $\rho_B^\theta = \text{tr}_A(|\psi_\theta\rangle\langle\psi_\theta|)$ is the reduced density matrix of the B system. The GI-Werner state has two free parameters θ and p , however its entanglement information only related to p . Like the Werner state, when $p > \frac{1}{3}$ it is entangled [28].

The second generalized Werner state, which we call the GII-Werner state, is

$$\rho(\theta, \phi) = p|\psi_{\theta, \phi}\rangle\langle\psi_{\theta, \phi}| + \frac{(1-p)I}{4}, \quad (10)$$

where, $|\psi_{\theta, \phi}\rangle = \cos\frac{\theta}{2}|00\rangle + e^{i\phi}\sin\frac{\theta}{2}|11\rangle$, $p \in (0, 1)$, $\theta \in (0, \pi)$, $\phi \in (0, 2\pi)$. The GII-Werner state has three free parameters θ , p and ϕ , but its entanglement information is only related to θ and p . It is entangled when $p > \frac{1}{(1+2\sin\theta)}$ [20].

Normally, it needs 15 observable operators to reconstruct a 2-qubits state density matrix. However, the

number of free parameters of above three quantum states is less than 15, and that of parameters related to entanglement may be even less. In principle, if we can effectively extract and process the entanglement information, we can classify the entanglement of quantum states with the least resource consumption.

We use the BCNN consisting of convolutional paths ($m \in \{1, 2, 3, 4\}; n_1 = 1, n_2 = 1$) and three fully connected layers to classify the entanglement of Werner state, GI-Werner state and GII-Werner state. The convolutional path used here has two convolutional layer, and each layer has just one kernel. It can train a observable operator and calculate its average. In practice, based on few observable operators, the BCNN can predict the entanglement of these quantum states with high accuracy, which shown in Fig.4(a). When classifying the entanglement of the Werner state, the accuracy of the BCNN achieve 99.7% with only one observable operator ($m = 1$). For the GI-Werner state, FC has achieved 97% accuracy with two selected observable operators [28] and BCNN can achieve 99.8% with only one observable operator ($m = 1$). For the GII-Werner state, BCNN can achieve 98.4% with two observable operators ($m = 2$) and 99.6% with three observable operators ($m = 3$), which is at the same level with the performance of FC with four selected observable operators [20]. (Compared with using a FC with four selected observable operators [20], our results are about the same.) The error distributions of the BCNN are shown in Fig.4(b-d). As we can see, the errors are concentrated on the boundary of entanglement and separability. Especially for GII-Werner state, the errors also occur when $\theta = 0$ and π , which there are only separable states. The trained observable operators which used to extract the entanglement information can be acquired from the kernels. We show them in TABLE I and only keep two decimal places.

Finally, we apply BCNN to classify the entanglement of general 2-qubits state. For the state generation, we adopt the method of $\rho = \frac{\sigma\sigma^\dagger}{\text{tr}(\sigma\sigma^\dagger)}$, where σ is a random complex matrix and keep the proportion of entangled states and separable states at 1:1. We show the performance of BCNN with three different convolutional path ($m = 1; n_1 = 4, n_2 = 4$), ($m \in [6, 15]; n_1 = 2, n_2 = 2$) and ($m \in [6, 15]; n_1 = 1, n_2 = 1$) in Fig.5. Since the general state is more complicated, we use five fully connected layers in BCNN. For the structure ($m = 1; n_1 = 4, n_2 = 4$), we fix one kernel in each convolutional layer as the identity matrix, and other kernels are still trainable. The outputs of the convolutional path are the averages of 15 observable operators and a constant 1. In this case, the accuracy of BCNN can achieve 97.5%. For ($m \in [6, 15]; n_1 = 2, n_2 = 2$), we also fix one kernel in each convolutional layer as the identity matrix. Each convolutional path outputs 3 observable operator averages and a constant 1. When $m \geq 9$, the convolutional paths are able to get all the information about the quantum state, and the accuracy of BCNN can be higher than 96.0%. For the structure ($m \in [6, 15]; n_1 = 1, n_2 = 1$),

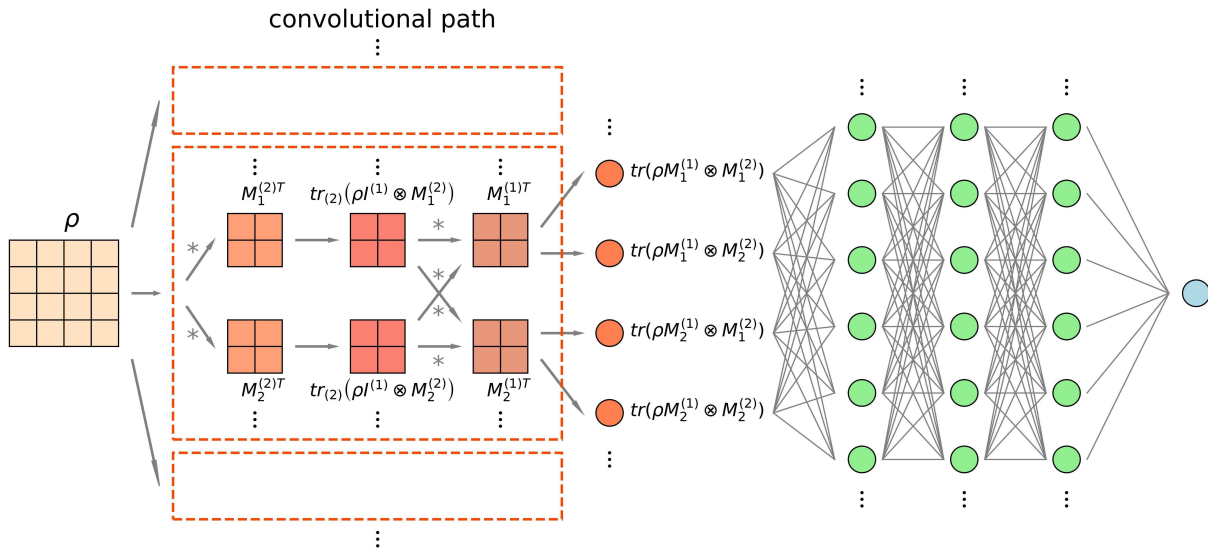


FIG. 3. Branching convolutional neural network(BCNN). The input of the network is the density matrix ρ , and it goes through several independent convolutional paths (showed in red dotted box). Every convolutional path has two convolutional layers and each convolutional layer has several kernels. Each convolutional path outputs the average of all combinations of the kernels of its two convolutional layers. Then, we take the outputs of these convolutional paths as the input of fully connected layer to classify the entanglement of states. For Werner, GI-Werner and GII-Werner states, we use three fully connected layers. For general 2-qubits state, we add two fully connected layers in the former structure.

TABLE I. Trained observable operators

state	operator number	$X^{(1)}$	$Y^{(1)}$	$Z^{(1)}$	$I^{(1)}$	$X^{(2)}$	$Y^{(2)}$	$Z^{(2)}$	$I^{(2)}$
Werer	1	-1.26	-0.97	-1.40	0.61	0.49	-0.18	1.63	0.62
GI-Werner	1	-0.37	0.16	1.08	0.19	-0.18	0.39	0.95	-0.51
	2	0.04	0.17	0.49	-1.57	-0.05	-0.22	1.00	-0.06
GII-Werner	2	-0.05	-0.09	1.39	0.07	0.02	0.22	0.97	0.17
		2.71	-0.27	0.50	0.56	2.40	-0.96	0.48	-0.53
	3	0.71	-1.23	-1.33	1.11	0.95	0.11	0.83	0.69
		-0.20	-0.64	-0.30	0.10	3.38	0.29	-0.25	-0.08

each convolutional path computes the average of just one observable operator. Therefore, with the increase of m , the accuracy of this structure raises lowest. And the BCNN still need 15 convolutional paths to extract all quantum state information and its accuracy can achieve 97.2%. In Fig.5(b), we show the error distribution of BCNN with three above convolutional paths when they are just able to extract all the information about quantum state. There only a few errors occur symmetrically around the boundary of entanglement and separability. As long as the structure of the convolutional paths allows all information to be extracted, the BCNN can train appropriate observable operators and detect the entanglement of a general quantum state with high accuracy, which is comparable to the results in article [20].

DISCUSSION

In this work, we prove the observable operator of discrete-level systems is a convolution kernel, which means that

the convolutional layer of artificial neural network can accurately calculate the average value of observable operator in quantum state, and that the Hermiticity of the convolutional layer can be maintained with the optimization algorithm based on gradient descent. With the foundation of above, we propose a BCNN, which can obtain well-trained observable operators to efficiently extract entanglement information and classify entanglement. We classify the entanglement of 2-qubits states, and studied the accuracy and the error distribution of BCNN.

We believe that CNN will be a promising tool for quantum physics. In our work, for Werner state, GI-Werner state and GII-Werner state, it can achieve 99.7%, 99.8%, and 98.4% respectively when the numbers of observable operators are same with that of parameters related to entanglement. It is superior to previous work in reducing resource consumption. For general 2-qubits state, our model still needs 15 observable operators to achieve the accuracy of 97.2%. In addition, we can extract the

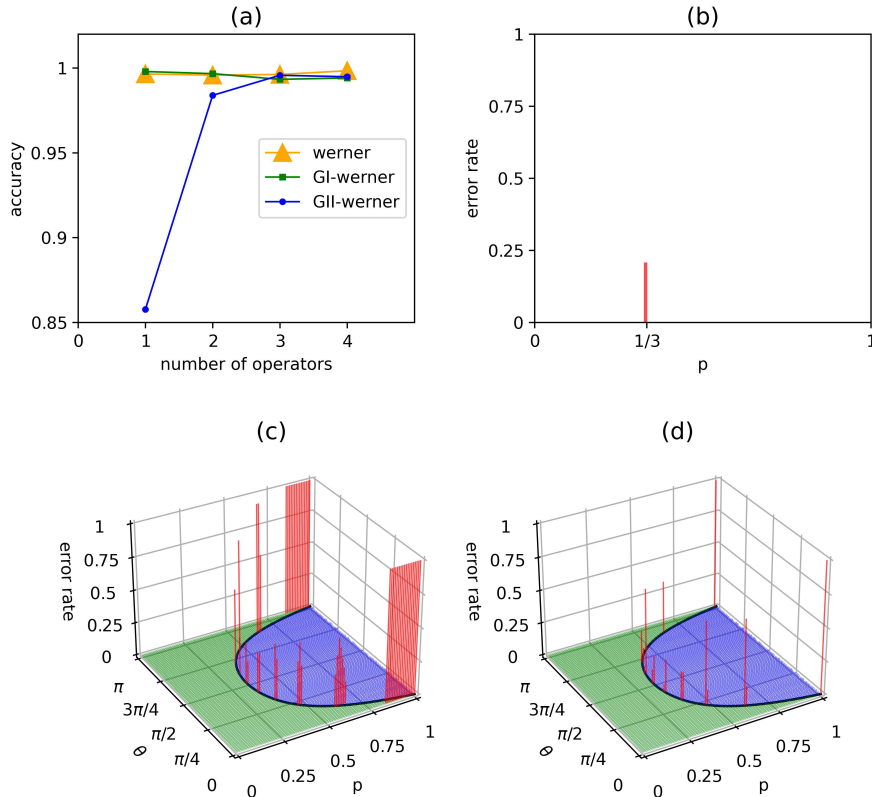


FIG. 4. **(a)**,The performance of BCNN for entanglement detection of Werner state, GI-Werner state and GII-Werner state. The accuracy increases with the number of observable operators. **(b)**,The error distribution of the BCNN with 1 observable operators, when entanglement classification is performed on GI-Werner state. When $p > \frac{1}{3}$, the state is entangled. And the errors concentrate on the boundary of entanglement and separability. **(c)(d)**,The error distribution of the BCNN with 2 and 3 observable operators, when entanglement classification is performed on GII-Werner state. We only drew the distribution when $\theta = 0, 0.1\pi, \dots, \pi$ for more clear view. The boundary of entanglement and separability is $p = \frac{1}{(1+2 \sin \theta)}$. And the errors concentrate on the boundary and the area $\theta = 0$ and π .

trained observable operators from kernels. These observable operators can be rewritten as the sum of the orthogonal normalization operators. We only keep two decimal places of the coefficient and input them into neural network to test again, and find that the accuracy of the BCNN almost keep the original level.

Since the convolutional layer can accurately calculate the average value of observable operator in quantum state, and this property applies to any dimension discrete-level system. It may be a powerful tool for solving measurement direction of the maximum violation of Bell inequality. We believe this property is likely to be used in other research and can bring new inspiration to the understanding of the relationship between quantum physics and artificial neural networks.

METHODS

The BCNN has several independent convolutional paths and fully connected layers. A convolutional path has several convolutional layers. The kernel of each convolutional layer represents the transpose of a observable operator acting on the system or subsystem. Therefore their convolutional layers should not have activation functions and biases. Each convolutional layer outputs all the averages of all combinations of the kernels of its convolutional layers. Then, we take the outputs of the convolutional paths as the input of fully connected layers for entanglement detection. And the structure of convolutional paths and fully connected layers should be adjusted according to the task. In this work, we use the BCNN consists of the convolutional paths ($m; n_1 = 1, n_2 = 1$) and three fully connected layers with the structure $(\alpha, 1024, 1)$ to detect the entanglement of Wenrer state, GI-Werner state

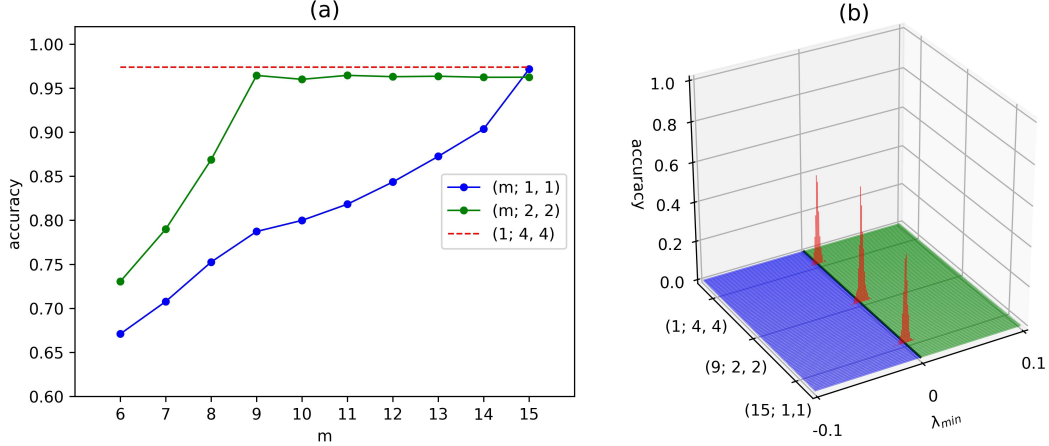


FIG. 5. **(a)**, The performance of BCNN for entanglement detection of 2-qubits general state. The accuracy almost increases linearly with the number of observable operators. **(b)**, The error distribution of the BCNN with 15 observable operators, when entanglement classification is performed on 2-qubits general state. The horizontal axis is the minimum eigenvalue λ_{min} . The error concentrates on the boundary of entanglement and separability. The error distribution is symmetric about the boundary, so our prediction is unbiased.

TABLE II. Adam parameters

state	operates number	lr	β_1	β_2	batch size	epoches
Werner	1-15	0.001	0.9	0.99	10	10
GI-Werner	1-15	0.001	0.35	0.99	10	10
GII-Werner	1	0.001	0.5	0.9	10	10
	2	0.001	0.9	0.99	200	30
General	3-15	0.001	0.375	0.99	10	10
	8	0.0003	0.325	0.825	400	20
	9	0.0003	0.325	0.85	400	20
	10	0.0003	0.325	0.87	400	20
	11	0.0003	0.325	0.9	400	20
	12	0.0003	0.325	0.95	400	20
	13	0.0003	0.325	0.925	400	20
	14	0.0003	0.325	0.925	400	20
15	0.0003	0.325	0.975	400	20	

and GII-Werner state. For general 2-qubits state, we test the BCNN consists of one of three different convolutional paths $(m; n_1 = 4, n_2 = 4)$, $(m; n_1 = 2, n_2 = 2)$ or $(m; n_1 = 1, n_2 = 1)$, and five fully connected layers $(\alpha, 1024, 1024, 1024, 1)$. The α is the number of the input nodes of the first fully connected layer, which is related to the structure of convolutional paths. The first layer has no activation functions and bias. The final layer's activation function is sigmoid and the loss function is cross entropy [55]. For other layers, we take Relu [56] as the activation function. We use Adam [57] as our optimizer to make it more likely to cross the saddle point and local minimum. We did not use the default recommended parameters of Adam, but adjust them according to the quantum state and the number of convolutional paths.

Our adam parameter settings are listed in TABLE II for reference.

In training process, we takes state density matrix as the input, and the kernels are initialized to a random Hermitian matrix. According to the features of the quantum state and the structure of convolutional paths, BCNN can automatically find appropriate observable operators for training task. In test process, we can directly calculate the average value of these trained observable operators, and input them into the following fully connected layers to detect entanglement. Of course, based on Eq.(1), single convolutional layer can be used to find global observable operators for entanglement detection, but the same task can already be completed by FC [50]. Therefore, in this article, we will focus on using two convolutional layers to express the product observable operator.

-
- [1] Carleo, G. & Troyer, M. Solving the quantum many-body problem with artificial neural networks. *Science* **355**, 602–606 (2016).
- [2] Torlai, G. *et al.* Neural-network quantum state tomography. In *Nature Physics* (2018).
- [3] Torlai, G. & Melko, R. G. Latent space purification via neural density operators. *Physical review letters* **120**, 240503.1–240503.5 (2018).
- [4] Melkani, A., Gneiting, C. & Nori, F. Eigenstate extraction with neural-network tomography. *Phys. Rev. A* **102**, 022412 (2020).
- [5] Carrasquilla, J., Torlai, G., Melko, R. G. & Aolita, L. Reconstructing quantum states with generative models. *Nature Machine Intelligence* **1**, 155–161 (2019).
- [6] Levine, Y., Sharir, O., Cohen, N. & Shashua, A. Quantum entanglement in deep learning architectures. *Physical Review Letters* **122**, 065001.1–065001.7 (2019).
- [7] Xiao, L. *et al.* Solving frustrated quantum many-particle models with convolutional neural networks. *Physical review. B* **98**, 104426.1–104426.6 (2018).
- [8] Choo, K., Neupert, T. & Carleo, G. Two-dimensional frustrated J_1 – J_2 model studied with neural network quantum states. *Phys. Rev. B* **100**, 125124 (2019).
- [9] Irikura, N. & Saito, H. Neural-network quantum states at finite temperature. *Phys. Rev. Research* **2**, 013284 (2020).
- [10] Stokes, J., Moreno, J. R., Pnevmatikakis, E. A. & Carleo, G. Phases of two-dimensional spinless lattice fermions with first-quantized deep neural-network quantum states. *Phys. Rev. B* **102**, 205122 (2020).
- [11] Liang, X., Dong, S.-J. & He, L. Hybrid convolutional neural network and projected entangled pair states wave functions for quantum many-particle states. *Phys. Rev. B* **103**, 035138 (2021).
- [12] Deng, D.-L., Li, X. & Das Sarma, S. Quantum entanglement in neural network states. *Phys. Rev. X* **7**, 021021 (2017).
- [13] Gao, X. & Duan, L.-M. Efficient representation of quantum many-body states with deep neural networks. *Nature Communications* **8** (2017).
- [14] Wang, L. Discovering phase transitions with unsupervised learning. *Phys. Rev. B* **94**, 195105 (2016).
- [15] Wang, C. & Zhai, H. Machine learning of frustrated classical spin models. i. principal component analysis. *Phys. Rev. B* **96**, 144432 (2017).
- [16] Ch’ng, K., Carrasquilla, J., Melko, R. G. & Khatami, E. Machine learning phases of strongly correlated fermions. *Phys. Rev. X* **7**, 031038 (2017).
- [17] Ohtsuki, T. & Ohtsuki, T. Deep learning the quantum phase transitions in random two-dimensional electron systems. *Journal of the Physical Society of Japan* **85**, 123706 (2016).
- [18] Ohtsuki, T. & Ohtsuki, T. Deep learning the quantum phase transitions in random electron systems: Applications to three dimensions. *Journal of the Physical Society of Japan* **86**, 044708 (2017).
- [19] Broecker, P., Carrasquilla, J., Melko, R. G. & Trebst, S. Machine learning quantum phases of matter beyond the fermion sign problem. *Scientific Reports* **7**, 8823 (2017).
- [20] Ma, Y. C. & Man-Hong, Y. Transforming bell’s inequalities into state classifiers with machine learning. *Npj Quantum Information* **4**, 34 (2017).
- [21] Lu, S. *et al.* Separability-entanglement classifier via machine learning. *Phys. Rev. A* **98**, 012315 (2018).
- [22] Gray, J., Banchi, L., Bayat, A. & Bose, S. Machine-learning-assisted many-body entanglement measurement. *Phys. Rev. Lett.* **121**, 150503 (2018).
- [23] Berkovits, R. Extracting many-particle entanglement entropy from observables using supervised machine learning. *Phys. Rev. B* **98**, 241411 (2018).
- [24] Qiu, P. H., Shi, X. G. & Shi, Y. W. Detecting entanglement with deep quantum neural networks. *IEEE Access* **PP**, 1–1 (2019).
- [25] Canabarro, A., Brito, S. & Chaves, R. Machine learning nonlocal correlations. *Phys. Rev. Lett.* **122**, 200401 (2019).
- [26] Kriv’chych, T. *et al.* A neural network oracle for quantum nonlocality problems in networks. *npj Quantum Information* **6** (2020).
- [27] Liu, Y. L., Wang, A. M., Sun, Y., Zhang, P. F. & Wang, G. D. Study on estimating quantum discord by neural network with prior knowledge. *Quantum Information Processing* **18** (2019).
- [28] Yang, M. *et al.* Experimental simultaneous learning of multiple nonclassical correlations. *Phys. Rev. Lett.* **123**, 190401 (2019).
- [29] Ren, C. & Chen, C. Steerability detection of an arbitrary two-qubit state via machine learning. *Phys. Rev. A* **100**, 022314 (2019).
- [30] Chen, C., Ren, C., Lin, H. & Lu, H. Entanglement structure detection via machine learning (2020). 2012.00526.
- [31] Deng, D.-L. Machine learning detection of bell nonlocality in quantum many-body systems. *Phys. Rev. Lett.* **120**, 240402 (2018).
- [32] Farhi, E., Goldstone, J. & Gutmann, S. A quantum approximate optimization algorithm (2014). 1411.4028.
- [33] Peruzzo, A. *et al.* A variational eigenvalue solver on a quantum processor. *Nature Communications* **5** (2013).
- [34] Amin, M. H., Andriyash, E., Rolfe, J., Kulchitsky, B. & Melko, R. Quantum boltzmann machine. *Phys. Rev. X* **8**, 021050 (2018).
- [35] Cong, I., Choi, S. & Lukin, M. Quantum convolutional neural networks. *Nature Physics* **15**, 1–6 (2019).
- [36] Grant, E. *et al.* Hierarchical quantum classifiers. *npj Quantum Information* **4** (2018).
- [37] Bennett, C. H. *et al.* Teleporting an unknown quantum state via dual classical and einstein-podolsky-rosen channels. *Phys. Rev. Lett.* **70**, 1895–1899 (1993).
- [38] Ekert, A. K. Quantum cryptography based on bell’s theorem. *Phys. Rev. Lett.* **67**, 661–663 (1991).
- [39] Raussendorf, R. & Briegel, H. J. A one-way quantum computer. *Phys. Rev. Lett.* **86**, 5188–5191 (2001).
- [40] Peres, A. Separability criterion for density matrices. *Phys. Rev. Lett.* **77**, 1413–1415 (1996).
- [41] Augusiak, R., Demianowicz, M. & Horodecki, P. Universal observable detecting all two-qubit entanglement and determinant-based separability tests. *Phys. Rev. A* **77**, 030301 (2008).
- [42] Rudolph, O. Further results on the cross norm criterion for separability. *Quantum Information Processing* **4** (2005).
- [43] Kai Chen, L.-A. W. A matrix realignment method for

- recognizing entanglement. *Quantum Information and Computation* **3**, 193–202 (2003).
- [44] Horodecki, M., Horodecki, P. & Horodecki, R. On the necessary and sufficient conditions for separability of quantum mixed states. *physics letters a* **223**, 1–8 (1996).
- [45] Wootters, W. K. Entanglement of formation of an arbitrary state of two qubits. *Phys. Rev. Lett.* **80**, 2245–2248 (1998).
- [46] Barbara, M. & Terhal. Bell inequalities and the separability criterion. *Physics Letters A* **271**, 319–326 (2000).
- [47] Rungta, P., Bužek, V., Caves, C. M., Hillery, M. & Milburn, G. J. Universal state inversion and concurrence in arbitrary dimensions. *Phys. Rev. A* **64**, 042315 (2001).
- [48] de Vicente, J. I. Lower bounds on concurrence and separability conditions. *Phys. Rev. A* **75**, 052320 (2007).
- [49] Gharibian, S. Strong np-hardness of the quantum separability problem. *Quantum Information and Computation* **10**, 343–360 (2010).
- [50] Yosefpor, M., Mostaan, M. R. & Raeisi, S. Finding semi-optimal measurements for entanglement detection using autoencoder neural networks. *Quantum Science and Technology* (2020).
- [51] Lecun, Y. & Bottou, L. Gradient-based learning applied to document recognition. *Proceedings of the IEEE* **86**, 2278–2324 (1998).
- [52] Ma, X., Tu, Z. C. & Ran, S.-J. Deep learning quantum states for hamiltonian estimation. *Chinese Physics Letters* **38**, 110301 (2021).
- [53] Horodecki, M., Horodecki, P. & Horodecki, R. Separability of mixed states: necessary and sufficient conditions. *Physics Letters A* **223**, 1–8 (1996).
- [54] Gühne, O. & Tóth, G. Entanglement detection. *Physics Reports* **474**, 1–75 (2009).
- [55] Dunne, R. A. & Campbell, N. A. On the pairing of the softmax activation and cross entropy penalty functions and the derivation of the softmax activation function. *Conf. on the Neural Networks* **185** (1997).
- [56] Glorot, X., Bordes, A. & Bengio, Y. Deep sparse rectifier neural networks. *Journal of Machine Learning Research* **15**, 315–323 (2011).
- [57] Kingma, D. & Ba, J. Adam: A method for stochastic optimization. *Computer Science* (2014).